Available online at www.sciencedirect.com

ScienceDirect

Procedia Engineering 81 (2014) 1318 – 1323

Procedia Engineering

www.elsevier.com/locate/procedia

11th International Conference on Technology of Plasticity, ICTP 2014, 19-24 October 2014, Nagoya Congress Center, Nagoya, Japan

Prediction of transient hardening after strain path change by a multi-scale crystal plasticity model with anisotropic grain substructure

Philip Eyckens[a]*, Albert Van Bael[a], Jaap Moerman[b], Henk Vegter[b], Paul Van Houtte[b]

[a]*Department of Metallurgy and Materials Engineering (MTM), Katholieke Universiteit Leuven, Kasteelpark Arenberg 44, 3001 Leuven, Belgium.*
[b]*Tata Steel, IJmuiden Technology Centre PO Box 10.000, 1970 CA, IJmuiden, The Netherlands.*

Abstract

Multi-scale modelling offers physical insights in the relationship between microstructure and properties of a material. The macroscopic anisotropic plastic flow may be accounted for by consideration of (a) the polycrystalline nature and (b) the anisotropic grain substructure. The latter contribution to anisotropy manifests itself most clearly in the event of a change in the strain path, as occurs frequently in multi-step forming processes. Under monotonic loading, both the crystallographic texture and the loading-dependent strength contribution from substructure influence the macroscopically observed strength.
The presented multi-scale plasticity model for BCC polycrystals combines a crystal plasticity model featuring grain interaction with a substructure model for anisotropic hardening of the individual slip systems. Special attention is given to how plastic deformation is accommodated: either by slip of edge dislocation segments, or alternatively by dislocation loop expansion.
Results of this multi-scale modelling approach are shown for a batch-annealed IF steel. Whereas both model variants are seen to capture the transient hardening after different types of strain path changes, the dislocation loop model offers more realistic predictions under a variety of monotonic loading conditions.

Selection and peer-review under responsibility of the Department of Materials Science and Engineering, Nagoya University

Keywords: Crystal plasticity; Texture; Substructure; Anisotropy; Transient hardening; Dislocation loop; IF steel

* Corresponding author. Tel.: +32 16 32 13 05; fax: +32 16 32 19 90.
E-mail address: Philip.eyckens@mtm.kuleuven.be

Selection and peer-review under responsibility of the Department of Materials Science and Engineering, Nagoya University
doi:10.1016/j.proeng.2014.10.150

1. Introduction

A strong effect of crystallographic texture on the anisotropic properties of polycrystals is widely recognized. Various texture-based crystal plasticity models have been developed and applied to forming process simulations, notably the prediction of earing profile in axisymmetric deep drawing operations, e.g. [1, 2]. State-of-the-art crystal plasticity models incorporate interaction effects between the constituting grains of the polycrystal. In this study, we adopt the Alamel crystal plasticity model [3], which considers grain-to-grain (short-range) interactions in a textured polycrystal. It has been demonstrated to be superior to the (full constraints) Taylor model regarding predictions of deformation texture [3], as well as the initial plastic anisotropy [4].

During continued plastic deformation of annealed polycrystals, another source of material anisotropy originates from the development of a complex and anisotropic dislocation patterning or grain substructure, cf. the review [5]. Several microscopic hardening models, including [6-9], have been proposed which consider the built-up of the dislocation substructure in order to capture the anisotropic hardening after strain path changes on a physical basis. In the present study, the anisotropic substructure model of [6] is adopted; it postulates a number of dislocation density evolution equations on the scale of the grain substructure, based on physical principles and TEM observations [10]. A distinction is made between three types of immobile dislocations: those contained within planar Cell Block Boundaries (CBBs) which cause latent hardening, those in-between the CBBs which cause isotropic hardening, and polarized (directionally mobile) dislocations at CBBs which lower the strength upon stress reversal.

The current study focuses on the anisotropic contribution of CBBs to the glide resistance of the available slip systems. In the next paragraph, an alternative formulation of this interaction is proposed, based on the assumption that slip is carried by the expansion of dislocation loops rather than slip of edge dislocation segments. Next, old and new model formulations are validated by flow stress prediction of tests with and without strain path changes, followed by general conclusions.

2. Model

In the present work, the dislocation substructural hardening model for polycrystals as detailed in [6] is largely followed, with 3 important exceptions:

- The iso-strain assumption of all constituting grains, as provided by the FC Taylor polycrystal model in [6], is abandoned. Instead, the interaction of neighboring grains (close-range interaction) is incorporated in the multi-scale modeling approach by means of the Alamel model [3].
- Polarization of the dislocation substructure is not considered in the present work. This condition is imposed in practice by setting the immobilization coefficient of polarized dislocations at Cell Block Boundaries (CBBs), denoted I^{wp} in [6], to 0.
- The dislocation type carrying the plastic slip as proposed in [6], is not necessarily followed (see below).

For every grain, the CRSS of each of the 24 {110}/{112}<111> slip systems *s* is given by:

$$\tau_s^{crit} = \tau_0 + (1 - f_{CBB})\alpha G b\sqrt{\rho} + f_{CBB}\ \sum_{i=1}^{6}\left(\alpha G b f_{i,s}^{geom}\sqrt{\rho_i^{wd}}\right), \tag{1}$$

in which $\alpha = 0.2$ is the dislocation interaction parameter, $G = 81.6$ GPa is the shear modulus and $b = 0.248$ nm is the magnitude of burgers vector. The first term, τ_0, is the friction stress in the dislocation-free lattice (a material parameter). The second term reflects the isotropic contribution to strength from both the statistically stored dislocations and the randomly oriented Cell Boundary (CB) network, as represented by the dislocation density ρ. The 3rd term represents the strength contribution from the planar Cell Block Boundaries (CBBs) *i*, oriented along one of the 6 (110)-planes and with dislocation density ρ_i^{wd}. A volume fraction of CBBs $f_{CBB} = 0.2$ is assumed. For the evolution equations of ρ and ρ_i^{wd}, it is referred to [6].

In [6], it is assumed that all slip is carried by edge dislocations, i.e. screw segments are neglected. The unit burgers vector $\mathbf{u_s^b}$ then denotes the (unique) dislocation flux direction of slip system *s*. The geometric screening factor of slip system *s* by CBBs of family *i* (with normal $\mathbf{u_i^n}$) is then given by:

$$f_{i,s}^{geom} \overset{\text{def}}{=} abs\left(\boldsymbol{u_s^b}.\boldsymbol{u_i^n}\right). \tag{2}$$

This assumption is called the 'edge dislocation model' further on. Note that Eq. (2) values to 0 (no interaction) if the burgers vector is parallel to the CBB, irrespective of the orientation of the slip plane.

A physically more sound assumption may be that slip is accommodated by the expansion of dislocation loops comprising of edge and screw segments with (generally) different mobility. However, as sketched in Fig. 1(a), the *dislocation flux in the slip plane* is in fact independent of the relative edge and screw mobility, as the dislocation density of edge or loop segments is inversely proportional to their respective mobility.

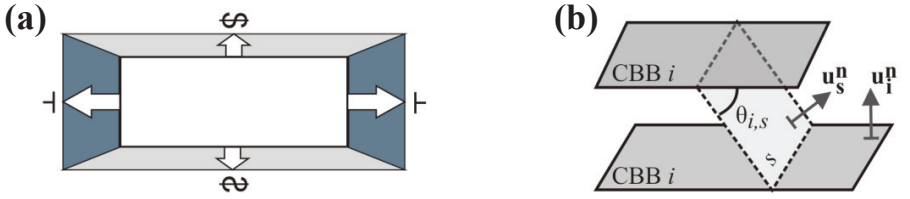

Fig. 1. Illustrations of the dislocation loop model: (a) Schematic of the expansion of a dislocation loop in its slip plane. The slipped area of edge segments (dark grey area) and screw segments (light grey area) are equal to each other, independently of the relative mobility of edge and screw segments; (b) The increase in slip resistance of an expanding dislocation loop on slip plane *s* due to the presence of CBBs of family *i*, is geometrically controlled by the relative orientation of slip plane normal $\mathbf{u_s^n}$ and CBB normal $\mathbf{u_i^n}$, as expressed by $f_{i,s}^{geom}$ in eq. (3).

For the 'dislocation loop model', eq. (2) is replaced by (see also Fig. 1(b)):

$$f_{i,s}^{geom} \overset{\text{def}}{=} sin\,\theta_{i,s} = \sqrt{1-(\boldsymbol{u_s^n}.\boldsymbol{u_i^n})^2}. \tag{3}$$

Note that eq. (3) values to 0 (no interaction) on the condition that the slip plane of *s* is parallel to the CBBs of *i*. As discussed in [11], the geometric screening factor of eq. (3) can also be interpreted as the ratio of the distance between two CBBs of one family *i* over the shortest distance between these CBBs within the slip plane *s*.

3. Results

Both models are applied to a batch-annealed IF deep-drawing steel (grade DC06) of 0.7 mm thickness. Its crystallographic texture features a sharp γ–fibre with partial α–fibre and is represented in the polycrystalline Alamel model [3] by a set of 4000 orientations (grains).

The 8 hardening parameters comprise the friction stress τ_0, the immobilization and recovery coefficients of ρ (I and R, resp.), the immobilization and recovery coefficients of ρ_i^{wd} for the currently generated CBBs (I^{wd} and R^{wd}, resp.), the recovery coefficient for homogeneous dissolution of non-currently-generated CBBs (R^{ncg}), and 2 heuristic parameters (β_1 and β_2) controlling the inhomogeneous dissolution of non-currently generated CBBs by micro shear band formation. For both models under consideration, the values given in Table 1 have been identified through curve fitting with experimental shear stress curves of simple shear tests, both on the undeformed material, as well as on 10% and 20% pre-rolled material, as shown in Fig. 2.

Table 1. Parameter sets.

Parameter:	τ_0 [MPa]	I [−]	R [m]	I^{wd} [−]	R^{wd} [m]	R^{ncg} [m]	β_1 [−]	β_2 [−]
Edge dislocation model:	54.1	2.75e-2	1.13e-9	4.21e-1	5.08e-9	5.62e-9	16.0	2.12e-2
Dislocation loop model:	57.3	2.97e-2	1.04e-9	5.90e-2	1.45e-9	6.21e-9	20.0	1.80e-3

As can be seen in Fig. 2, a reasonable overall fit is obtained for both models, including the transient softening after orthogonal strain path changes (graphs on the right).

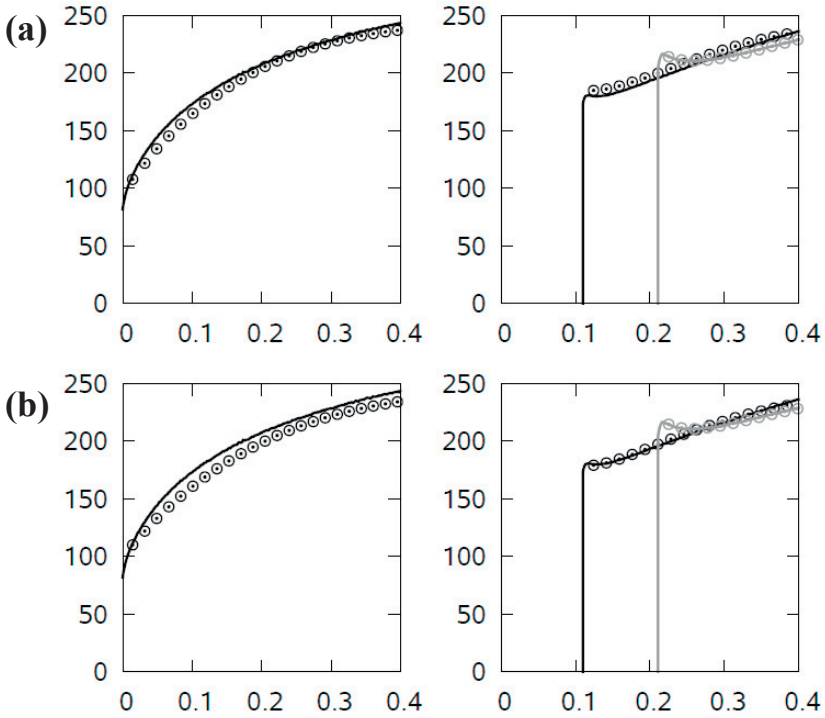

Fig. 2. Result of hardening parameter identification for (a) edge dislocation model; (b) dislocation loop model. On Y-axis, the shear stress is plotted (unit: MPa). On X-axis, the von Mises equivalent strain is plotted (unit: /). The left graphs show simple shear loading without prestrain; the right graphs show shear loading on 10% and 20% pre-rolled material along RD. Simple shear direction is in each case along TD. Experimental curves: full line; Model curves: symbols.

Fig. 3 presents predictions of both calibrated models for strain path change loadings with Schmitt-Aernoudt-Baudelet factor of 0.5 (i.e. in-between an orthogonal loading and strain path continuation). Both models can capture the strain path softening and reproduce adequately the strength increase with increasing pre-strains. On the basis of validation tests presented in Fig. 3, both models are seen to have a comparable accuracy.

The models have been identified purely on simple shear loading (without and with pre-strain). In Fig. 4, predictions of the models are made for other loading deformation on as-received materials, being uniaxial tensile loading along RD (‘tens’) and uniaxial compression loading along ND on a stack of sheet material. For the latter loading, the experimental methodology of [12] has been followed. This kind of validation is relevant since the build-up of CBB substructure also contributes to the strength under monotonic loading conditions, as can be seen in eq. (1). For γ–fibre textured materials such as the presently considered IF steel, the CBB development is loading-dependent, leading e.g. to different work hardening under uniaxial (‘tens’) and equibiaxial (‘compr’) loading [13].

In Fig. 4, it is seen that the quality of the two models are fairly similar for tensile loading (‘tens’). The prediction of the compressive loading along ND (‘compr’) is however significantly better for the dislocation loop model (though not perfect) as compared to the edge dislocation loop model. This result supports the claim that consideration of dislocation loop expansion of individual slip systems is a more physically sound assumption than assumption of slip carried solely by edge dislocation segments.

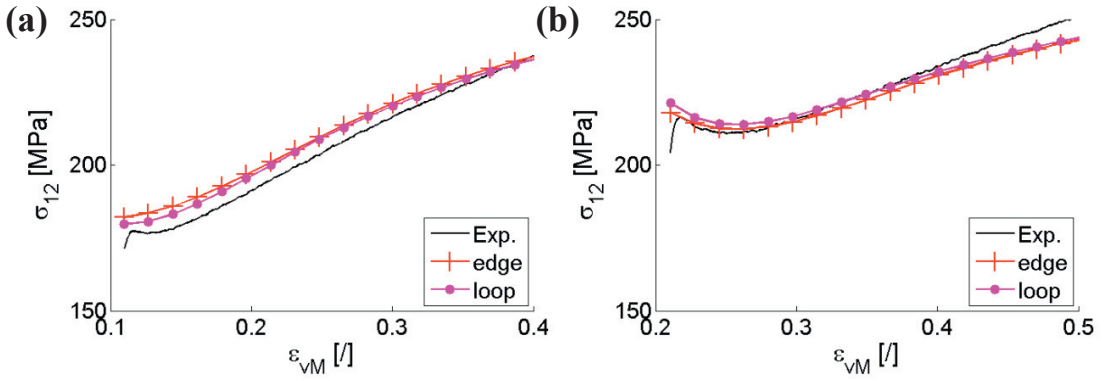

Fig. 3. Experimental and predicted stress-strain curves under simple shear loading (shear direction at 135° to RD) after (a) 10% rolling pre-strain along RD; (b) 20% rolling pre-strain along RD. On Y-axis, the shear stress is plotted (unit: MPa). On X-axis, the von Mises equivalent strain is plotted. Experimental curves: full line; Edge dislocation model: full line with '+' symbol; (b) dislocation loop model: full line with '●' symbol.

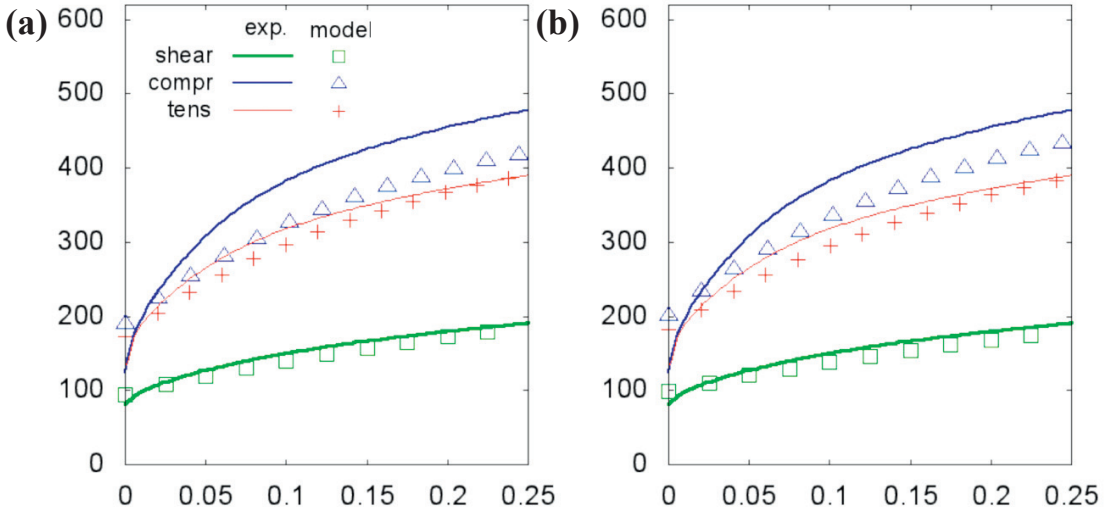

Fig. 4. Experimental and predicted stress-strain curves under various monotonic loading cases for (a) edge dislocation model; (b) dislocation loop model. On Y-axis, the shear/compression/tensile stress is plotted (unit: MPa). On X-axis, the shear/compression/tensile strain is plotted (unit: /). Experimental curves: full line; Model curves: symbols.

4. Discussion

Based on the similar accuracy of both hardening models observed in Figs. 2 and 3 it appears that, once a suitable parameter set has been obtained by curve-fitting to the polycrystalline stress-strain response for both (a) continued loading (no strain path change) and (b) orthogonal loading cases, a reasonably accurate prediction of the stress response in an intermediate loading case can be obtained in a manner that is quite insensitive to the interaction assumptions within the model. For these assumptions, which may describe the physical processes only in a poorly manner, the parameter identification procedure by curve fitting can apparently compensate for the lack of physical soundness. Significantly different loading conditions than those used in the identification procedure, such as those of Fig. 4, thus present a more valuable model valorization and evaluation of the underlying assumptions regarding physical processes that form the basis of strain hardening. Whereas the dislocation loop model is seen to be closer

to experimental behavior then the edge dislocation model, future refinement of the modeling approach appears in order, notably regarding (i) the physical processes that are the origin of the development of the dislocation substructure with progressive deformation, and (ii) the contribution of the developed substructure to slip resistance on the individual slip systems.

5. Conclusion

For one IF steel, this study examined in detail two variants of dislocation substructural hardening model, with different assumptions on the nature of the dislocation type accommodating plastic slip and corresponding interactions with planar substructural features (cell bock boundaries). Improvement in the physical description has been attained by replacing the assumption of slip carried by edge dislocation segments, with the assumption of slip carried by dislocation loop expansion. The modelling improvement is in particular seen for loading conditions that are very different to those for which the set of hardening parameters has been identified.

Acknowledgements

This research was carried out under the project number M41.10.08307b in the framework of the Research Program of the Materials innovation institute M2i (www.m2i.nl). Jerzy Gawad is kindly acknowledged for providing software to calculate the material response for the stress-driven loadings in Fig. 4.

References

[1] Engler, O. and J.r. Hirsch, Polycrystal-plasticity simulation of six and eight ears in deep-drawn aluminum cups. Materials Science and Engineering: A, 2007. 452-453(0): 640-651.
[2] Gawad, J., A. Van Bael, P. Eyckens, G. Samaey, P. Van Houtte, and D. Roose, Hierarchical multi-scale modeling of texture induced plastic anisotropy in sheet forming. Computational Materials Science, 2013. 66(0): 65-83.
[3] Van Houtte, P., S. Li, M. Seefeldt, and L. Delannay, Deformation texture prediction: from the Taylor model to the advanced Lamel model. International Journal of Plasticity, 2005. 21(3): 589-624.
[4] Eyckens, P., Q. Xie, J.J. Sidor, L. Delannay, A. Van Bael, L. Kestens, J. Moerman, H. Vegter, and P. Van Houtte. Validation of the texture-based ALAMEL and VPSC models by measured anisotropy of plastic yielding. in Materials Science Forum 702-703 (Proc. of ICOTOM 16). 2011. Mumbai, India: Trans Tech Publications.
[5] Hansen, N. and D. Juul Jensen, Deformed metals – structure, recrystallisation and strength. Materials Science and Technology, 2011. 27(8): 1229-1240.
[6] Peeters, B., M. Seefeldt, C. Teodosiu, S.R. Kalidindi, P. Van Houtte, and E. Aernoudt, Work-hardening/softening behaviour of b.c.c. polycrystals during changing strain paths: I. An integrated model based on substructure and texture evolution, and its prediction of the stress-strain behaviour of an IF steel during two-stage strain paths. Acta Materialia, 2001. 49(9): 1607-1619.
[7] Hamelin, C.J., B.J. Diak, and A.K. Pilkey, Multiscale modelling of the induced plastic anisotropy in bcc metals. International Journal of Plasticity, 2011. 27(8): 1185-1202.
[8] Lee, M.G., H. Lim, B.L. Adams, J.P. Hirth, and R.H. Wagoner, A dislocation density-based single crystal constitutive equation. International Journal of Plasticity, 2010. 26(7): 925-938.
[9] Rauch, E.F., J.J. Gracio, F. Barlat, and G. Vincze, Modelling the plastic behaviour of metals under complex loading conditions. Modelling and Simulation in Materials Science and Engineering, 2011. 19(3): 035009.
[10] Peeters, B., B. Bacroix, C. Teodosiu, P. Van Houtte, and E. Aernoudt, Work-hardening/softening behaviour of b.c.c. polycrystals during changing strain: : Part II. TEM observations of dislocation sheets in an IF steel during two-stage strain paths and their representation in terms of dislocation densities. Acta Materialia, 2001. 49(9): 1621-1632.
[11] Li, Z.J., G. Winther, and N. Hansen, Anisotropy in rolled metals induced by dislocation structure. Acta Materialia, 2006. 54(2): 401-410.
[12] An, Y.G. and H. Vegter, Analytical and experimental study of frictional behavior in through-thickness compression test. Journal of Materials Processing Technology, 2005. 160(2): 148-155.
[13] Uenishi, A., N. Sugiura, Y. Ikematsu, S. Masaaki, E. Isogai, and S. Hiwatashi. Work Hardening Behaviour and Dislocation Patterning at Large Strains in Sheet Steel. in Proceedings of the 2nd International Symposium on Steel Science. 2009. Kyoto, Japan: The Iron and Steel Institute of Japan. 57-62.